SHORT COMMUNICATION

Load flow solution with induction motor

Pichai Aree[1]

Abstract

Aree, P.
Load flow solution with induction motor
Songklanakarin J. Sci. Technol., 2006, 28(1) : 157-168

The classical constant-power load model is usually employed for load flow analysis. Since the actual loads of power systems mostly have nonlinear voltage-dependent characteristics, integration of nonlinear load models into load flow algorithm is essential to get better and accurate results of load flow analysis. In this paper, the conventional load flow algorithm is modified to incorporate the nonlinear model of induction motor load. The algorithm efficiency of the modified load flow has been investigated using the IEEE-30bus standard system. The results show that the induction motor loads have significant impacts on convergence characteristics of active and reactive power mismatches of the modified load flow.

Key words : load flow analysis, induction motor

[1]**Ph.D.(Electrical Engineering), Asst. Prof., Department of Electrical Engineering, Faculty of Engineering, Thammasat University, Rangsit, Khlong Luang, Pathum Thani, 12120 Thailand.**
E-mail: apichai@engr.tu.ac.th
Received, 4 February 2005 Accepted, 14 June 2005

บทคัดย่อ

พิชัย อารีย์

ผลเฉลยโหลดโฟลว์ร่วมกับมอเตอร์เหนี่ยวนำ

ว. สงขลานครินทร์ วทท. 2549 28(1) : 157-168

แบบจำลองของโหลดชนิดกำลังคงที่ (constant-power load) โดยทั่วไปจะใช้ในการวิเคราะห์โหลดโฟลว์ (load flow) ของระบบไฟฟ้ากำลัง แบบจำลองนี้อาจไม่เหมาะสม เพราะค่ากำลังไฟฟ้าของโหลดส่วนใหญ่ในระบบไฟฟ้ากำลังมีค่าแปรตามขนาดของแรงดันในลักษณะไม่เชิงเส้น (nonlinear voltage dependent load) ดังนั้นการนำแบบจำลองโหลดชนิดนี้ร่วมกับโหลดโฟลว์อัลกอริทึม (load flow algorithm) จึงมีความสำคัญเพื่อให้ผลลัพธ์ของการวิเคราะห์โหลดโฟลว์มีความถูกต้องมากขึ้น งานวิจัยนี้ได้เสนอแนวทางใหม่ในการปรับปรุงโหลดโฟลว์อัลกอริทึม โดยการผนวกแบบจำลองไม่เชิงเส้นของโหลดมอเตอร์เหนี่ยวนำ (induction motor) เข้ากับโหลดโฟลว์อัลกอริทึมแบบเดิม ประสิทธิภาพของโหลดโฟลว์อัลกอริทึมที่ปรับปรุงใหม่นี้ได้รับการทดสอบโดยใช้ระบบทดสอบมาตรฐานสามสิบบัสของไอสามอี (IEEE 30bus system) จากการศึกษาพบว่ามอเตอร์เหนี่ยวนำมีผลกระทบต่อลักษณะการลู่เข้าหาคำตอบ (convergence characteristic) ของโหลดโฟลว์ที่ได้รับการปรับปรุง โดยพิจารณาจากค่าความคลาดเคลื่อนของกำลังไฟฟ้าแอ็กทิฟและรีแอ็กทิฟ (active and reactive power mismatches)

ภาควิชาวิศวกรรมไฟฟ้า คณะวิศวกรรมศาสตร์ มหาวิทยาลัยธรรมศาสตร์ ศูนย์รังสิต อำเภอคลองหลวง จังหวัดปทุมธานี 12120

Power flow calculations provide a starting point for most power system analysis. For example, the problems related to transient and voltage stabilities due to dynamic behavior of induction motor loads have been a major area of attraction for power system planners and operation engineers all over the world. The fundamental investigations have based on the steady-state analysis using conventional power flow (Herley *et al*., 1988; IEEE task force, 1995; Prasad *et al*., 1997; Liu *et al*., 1997). The scheduled active and reactive powers of induction motors are input parameters for a given initial terminal voltage (1.0pu). Both active and reactive powers are kept constant during the load flow iteration since loads are considered as constant power (IEEE task force, 1993). After the load flow successfully converges, the scheduled active power and the obtained terminal voltage are employed to compute the actual values of slip and reactive power of the motors. The difference between the actual and scheduled reactive powers is resolved by adding the shunt reactive power compensation (IEEE task force, 1995; Pereira *et al*., 2002). For instance, if the actual reactive power of the motor is greater than the scheduled reactive power, the compensating capacitor will be calculated and placed at the motor terminal bus. This initializing method may not give the exact value of motor reactive power consumption and may not yield a meaningful analysis for the voltage and transient stability studies.

In this paper, the conventional load flow algorithm has been upgraded and modified to incorporate the nonlinear characteristics of induction motor load. The modified load flow accounts for the motor slip and scheduled reactive power that are adjusted during the iteration process. The impacts of induction motors on the convergence characteristics of load flow are investigated using the IEEE-30bus standard test system (Wallach, 1986).

1. Slip and reactive power calculations of induction motor

The induction motor is represented by a standard equivalent single-cage model (Kundur, 1993) as shown in Figure 1, where R_s and R_r are stator and rotor resistances, X_{ls} and X_{lr} are stator and rotor leakage reactances. X_m is magnetizing reactance. All these parameters are referred to

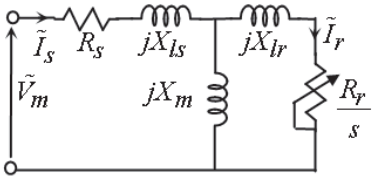

Figure 1. Equivalent circuit of single-cage induction motor

stator side.

According to Figure 1, the input active power of induction motor can be expressed by,

$$P_m = I_s^2 R_s + I_r^2 R_r / s \tag{1}$$

Where,

$$I_s = V_m \sqrt{\frac{(R_r / s)^2 + X_{lr}^2}{\left((R_{th} + R_r / s)^2 + (X_{th} + X_{lr})^2\right)\left(R_s^2 + X_{lr}^2\right)}} \tag{2}$$

$$I_r = \frac{V_m X_m}{\sqrt{\left((R_{th} + R_r / s)^2 + (X_{th} + X_{lr})^2\right)\left(R_s^2 + X_{lr}^2\right)}} \tag{3}$$

$$R_{th} = \frac{R_s X_m^2}{R_s^2 + (X_m + X_{ls})^2} \tag{4}$$

$$X_{th} = \frac{R_s^2 X_m + X_m X_{ls}(X_m + X_{ls})}{R_s^2 + (X_m + X_{ls})^2} \tag{5}$$

After substituting (2) and (3) into (1), the motor slip may be written in form of the quadratic equation by,

$$s^2 + bs + c = 0 \tag{6}$$

Where

$$b = \frac{R_r\left(2P_m R_s X_m^2 - V_m^2 X_m^2\right)}{P_m\left((X_m^2 - X_{lr}X_{ls})^2 + (R_s X_{lr})^2\right) - V_m^2 R_s X_{lr}^2} \tag{7}$$

$$c = \frac{R_r^2\left((R_s^2 + X_{ls}^2)P_m - V_m^2 R_s\right)}{P_m\left((X_m^2 - X_{lr}X_{ls})^2 + (R_s X_{lr})^2\right) - V_m^2 R_s X_{lr}^2} \tag{8}$$

According to Figure 1, the complex apparent power drawn by induction motor can be expressed as function of voltage and slip by,

$$\tilde{S}_m = \tilde{V}_m (\tilde{I}_m)^* \tag{9}$$

Where

$$\tilde{I}_m = \frac{\tilde{V}_m}{R_{mot} + jX_{mot}} \tag{10}$$

$$R_{mot} = R_s + \frac{X_m^2 (R_r / s)}{(R_r / s)^2 + (X_m + X_{lr})^2} \tag{11}$$

$$X_{mot} = X_{ls} + \frac{X_m (R_r / s)^2 + X_m X_{lr}(X_m + X_{lr})}{(R_r / s)^2 + (X_m + X_{lr})^2} \tag{12}$$

The motor reactive power consumptions, imaginary component of (9), are given by,

$$Q_m = \frac{V_m^2 X_{mot}}{(R_{mot})^2 + (X_{mot})^2} \tag{13}$$

2. Modified Newton-Raphson load flow algorithm

In the conventional load flow study, the active and reactive powers of all load buses are generally specified. A constant-power load model is usually used for representing the load buses. Hence, these active and reactive powers are independent of the deviation of voltage magnitude. To solve the load flow equations with induction motor loads, the motor active power can be practically assumed to be fairly constant (Machowski *et al*., 1997). This assumption is valid when the motors are operated in the vicinity of small changes of the supply voltage, not below the stalling point. With this assumption, the scheduled active powers of motor load buses are kept constant during the load flow iteration process. Although the constant-power model is applicable for the active power, it may not suitable for the reactive power consumption of motors because the reactive power is very sensitive to the voltage variations (Machowski *et al.,* 1997). Therefore, the correct way to solve

the load flow problem with induction motor loads is to update its reactive power and slip for every each iteration. Their slips and reactive powers can be calculated from (6) and (13), respectively. The procedure for the Newton-Raphson load flow analysis with the induction motors can be summarized as follows:

Step 1: Read bus data, line impedance data, transformer data, induction motor parameters, numbers and rating of motors, etc.
Step 2: Initialize voltages and angles at all buses.
Step 3: Construct admittance matrix.
Step 4: Set iteration count $k = 0$.
Step 5: Calculate real and reactive bus powers.
Step 6: Calculate difference between scheduled and calculated powers.

$$\Delta P^{(k)} = P_{(scheduled)} - P^{(k)}_{(calculated)}$$

$$\Delta Q^{(k)} = Q_{(scheduled)} - Q^{(k)}_{(calculated)}$$

For the induction motor load bus, $Q_{(scheduled)}$ can be calculated by using (13) after slip is found from (6).

Step 7: Build the conventional Jacobian matrix.
Step 8: Solve Jacobian equation for voltage and angle.
Step 9: Update voltages and angles.
Step 10: Check power mismatches. If power mismatches are satisfied, the power flow solution can be found, and then terminate the process.
Step 11: Set $k = k + 1$ and if $k < k_{max}$, go to step 5, otherwise terminate the process.

3. Load Flow Test Case

In this section, the IEEE-30bus standard network was used in order to show, quantitatively, how the modified load flow with the induction motor load performed. The solution details are provided so as to enable the potential reader to make any comparison. The network configuration is shown in Figure 2 and its data are given in Table A1-A5 of Appendix A. In this study, the network was modified to include 25 horsepower (HP) induction motors at bus 26. The motor's data are

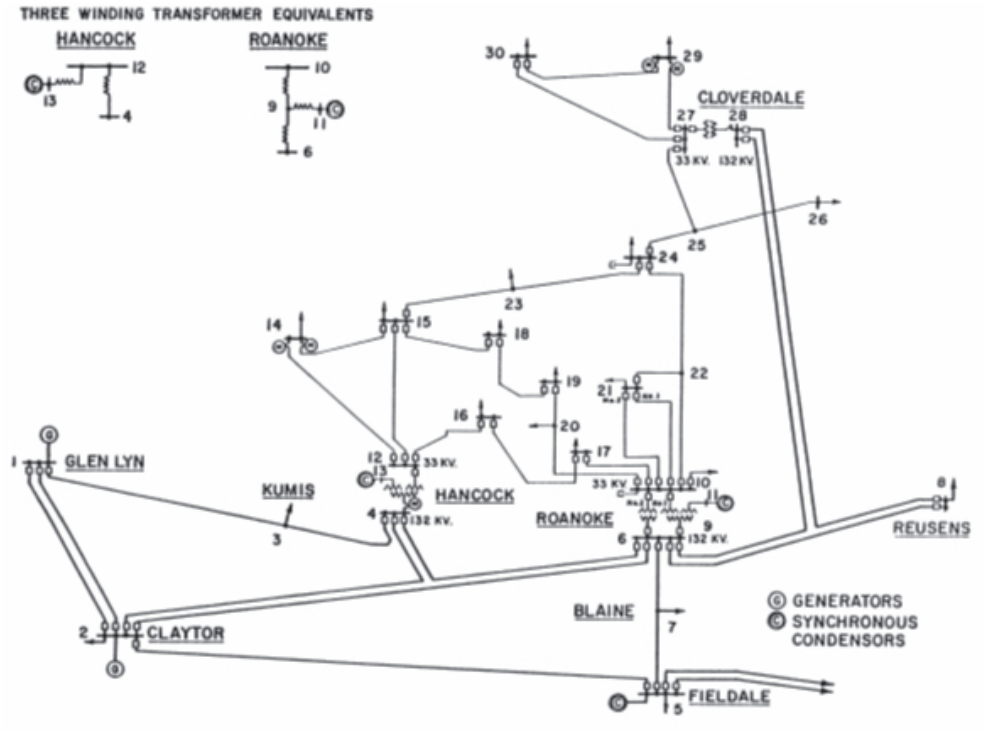

Figure 2. IEEE-30bus system.

Table 1. Final converged load flow solution.

Bus no.	Voltage (pu)	Angle (deg)	Generation		Load	
			MW	MVAR	MW	MVAR
1	1.0600	0	261.038	-15.431	0.000	0.000
2	1.0426	-5.4953	40.0	50.000	21.70	12.70
3	1.0200	-7.9878	0.00	0.00	2.400	1.200
4	1.0110	-9.6430	0.00	0.00	7.600	1.600
5	1.0100	-14.404	0.00	37.558	94.20	19.00
6	1.0095	-11.372	0.00	0.00	0.000	0.000
7	1.0019	-13.144	0.00	0.00	22.80	10.90
8	1.0100	-12.135	0.00	39.399	30.00	30.00
9	1.0459	-14.422	0.00	0.00	0.000	0.000
10	1.0415	-16.020	0.00	0.00	5.800	2.000
11	1.0700	-14.422	0.00	12.414	0.000	0.000
12	1.0556	-15.313	0.00	0.00	11.20	7.500
13	1.0700	-15.313	0.00	10.992	0.000	0.000
14	1.0406	-16.205	0.00	0.00	6.200	1.600
15	1.0358	-16.289	0.00	0.00	8.200	2.500
16	1.0424	-15.885	0.00	0.00	3.500	1.800
17	1.0365	-16.187	0.00	0.00	9.000	5.800
18	1.0256	-16.892	0.00	0.00	3.200	0.900
19	1.0228	-17.058	0.00	0.00	9.500	3.400
20	1.0267	-16.856	0.00	0.00	2.200	0.700
21	1.0293	-16.468	0.00	0.00	17.50	11.20
22	1.0299	-16.455	0.00	0.00	0.000	0.000
23	1.0251	-16.674	0.00	0.00	3.200	1.600
24	1.0192	-16.842	0.00	0.00	8.700	6.700
25	1.0166	-16.431	0.00	0.00	0.000	0.000
26	**1.0005**	**-16.911**	**0.00**	**0.00**	**3.498**	**1.876**
27	1.0226	-15.890	0.00	0.00	0.000	0.000
28	1.0062	-12.003	0.00	0.00	0.000	0.000
29	1.0027	-17.121	0.00	0.00	2.400	0.900
30	0.9913	-18.005	0.00	0.00	10.60	1.900

given in Appendix B. The scheduled active power (P_m) at bus 26, as indicated by Table A5, was 3.498MW. It was calculated from the individual sum of 165 numbers of the 25HP-motor input powers at the rated voltage. This active power was kept constant during the iteration process. On the other hand, the scheduled reactive power (Q_m) of the motors was initially calculated using (13) with the flat voltage profile (V_m = 1.0pu). This reactive power was adjusted every each iteration. After the load flow study successfully converged to the mismatch tolerance of $1.0E^{-10}$, the final iterative solutions are summarized in Table 1. The motor terminal voltage (1.0005pu) and reactive power (1.876MVAR) at bus 26 were obtained as well as the converged slip (0.05827). The modified load flow calculation gives the exact amount of the reactive power required by the induction motor loads. Thus, any artificial admittance added into the motor load bus is not necessary for adjusting the difference between the actual and scheduled reactive powers, when the voltage and transient stabilities are analyzed.

4. Convergence Test

In this section, the load flow convergence characteristics are investigated using the IEEE-30bus system. The behavior of the maximum absolute mismatches of active and reactive powers of the test system is shown in Figure 3 as a function of iteration numbers. Both active and reactive power mismatches (ΔP and ΔQ) of all buses except the reactive power mismatch of bus 26 converged rapidly to the target tolerance of $1.0E^{-10}$ in 5 iterations. However, the iteration process did not stop because of the large value of reactive power mismatch at bus 26. This power mismatch was the key factor that greatly influenced the number of iterations. The solutions of the modified power flow slowly converged in 9 iterations, starting from a flat voltage profile, after the reactive power mismatch was below the specified tolerance ($1.0E^{-10}$). The convergence characteristics of both conventional and modified load flows were also compared. The power demands of all load buses obtained from the modified load flow were re-simulated using the conventional load flow. The absolute mismatch characteristics of the conventional and modified load flows are shown in Figure 4. It is apparent that the quadratic convergence

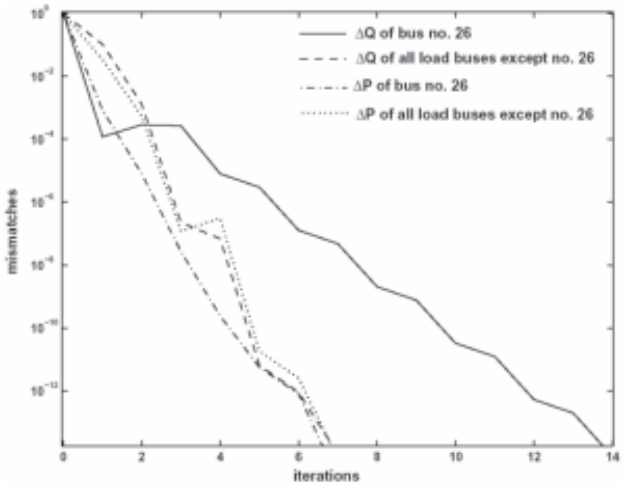

Figure 3. Active and reactive power mismatches of modified load flow

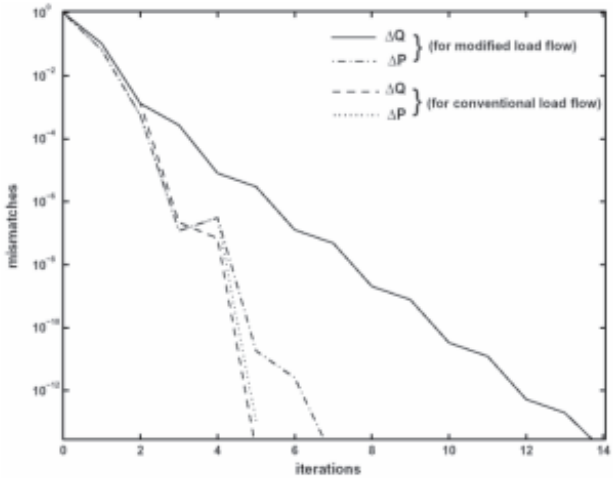

Figure 4. Active and reactive power mismatches of conventional and modified load flows

characteristics of the conventional load flow were preserved, but those of the modified load flow were lost. The reactive power mismatch of bus 26 converged in the linear manner due to the adjustments of motor's slip and reactive power during the Newton-Raphson iteration process. Thus, at the tolerance of $1.0E^{-10}$, the modified load flow required a greater number of iterations almost twice than that of the conventional load flow. It can be seen that the reactive and slip adjustments cause a significant degrading in the convergence characteristics.

The effects of induction motors on the load flow convergence characteristics were further explored when the load buses (*PQ* buses) of IEEE-30bus network were integrated with the motors. First, the critical load buses, having the biggest influences on the load flow convergence and voltage collapse, were identified to incorporate the motors. The *Q*-*V* sensitivity analysis (Kundur, 1993) was employed to compute the eigenvalues of the *PQ*-bus Jacobian and their participation factors. The eigenvalues of all load buses are listed in Table 2. It is noted that the maximum computed eigenvealues indicate the most important mode. The participation factors of the first two critical modes (1.9777 and 0.9684) were computed and plotted in Figures 5 and 6, respectively. It can be seen that the significant load buses related to the critical modes 1 and 2 were 23, 24, 26, 29, 30 and 10, 14-21, respectively. The study was conducted by adding the motors into these selected buses.

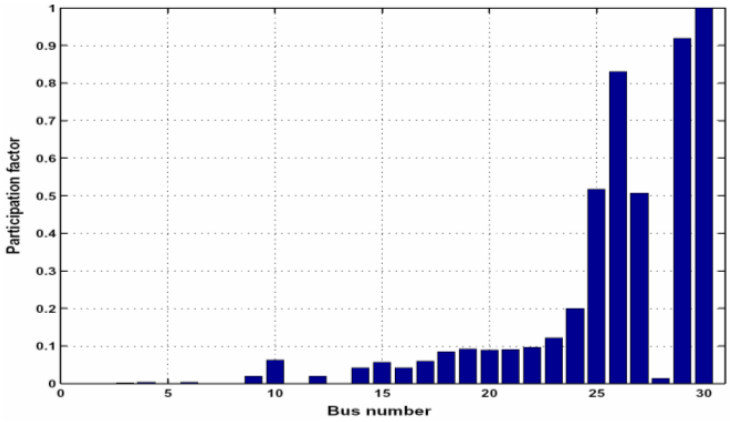

Figure 5. Participation factors of the eigenvalue (1.9777)

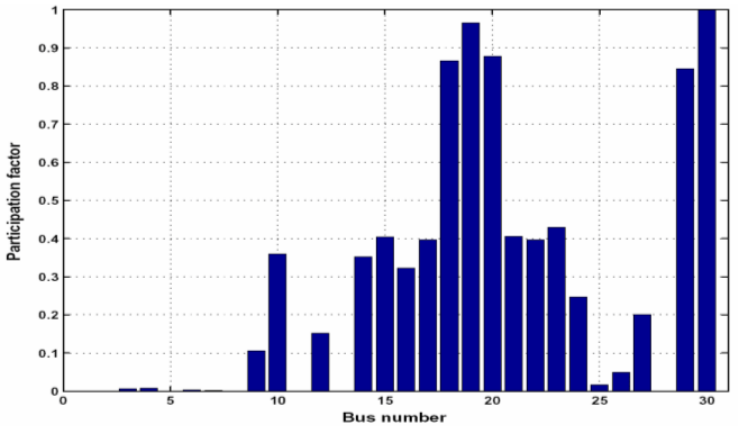

Figure 6. Participation factors of the eigenvalue (0.9684)

Table 2. Critical eigenvalues of all load buses.

Mode	Eigenvalues	Mode	Eigenvalues
1	**1.9777**	13	0.0599
2	**0.9684**	14	0.0551
3	0.5585	15	0.0521
4	0.2781	16	0.0506
5	0.2461	17	0.0431
6	0.1814	18	0.0426
7	0.1593	19	0.0287
8	0.1313	20	0.0282
9	0.1136	21	0.0264
10	0.0970	22	0.0168
11	0.0731	23	0.0148
12	0.0723	24	0.0099

Ten percent of the scheduled active powers, shown in Table A5, were allocated for the motor loads at these buses. The reactive power mismatches of the conventional (case *a*) and modified (cases *b, c, d*) load flows are displayed in Figure 7. The case *b* related to the situation in which a group of 25HP motors was only implemented into the most critical bus 30 with highest computed participation factor. In cases *c* and *d*, a group of 25HP motors was integrated into the load buses that were connected to the mode 1 and modes 1 plus 2, respectively. Figure 7 shows a significant increase in the number of iterations as the motors were at first added to the critical bus 30 (case *b*). It was only slightly increased after the motors were incorporated into the other related buses (cases *c* and *d*).

The study was carried out to investigate the convergence characteristics when the portions of motors at bus 26 were increased from 0 to 100 percents (3.498MW). The plots of the active and reactive power mismatches are shown in Figure 8. The letters *p* and *q* denote active and reactive power mismatches, respectively. As the portions of motors were increased from 20 to 100%, the

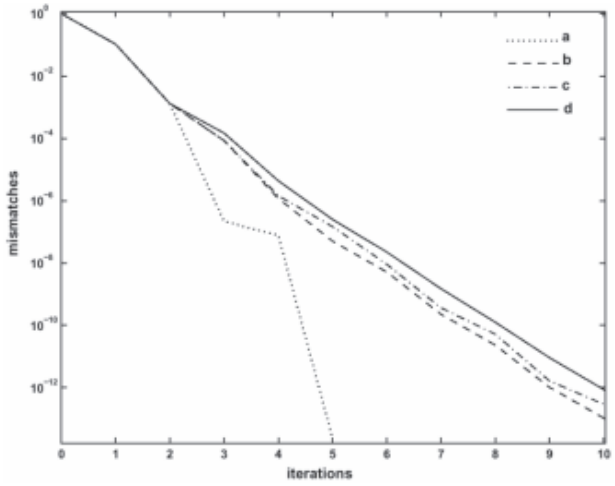

Figure 7. Reactive power mismatches of modified load flow with increased number of motor load buses.

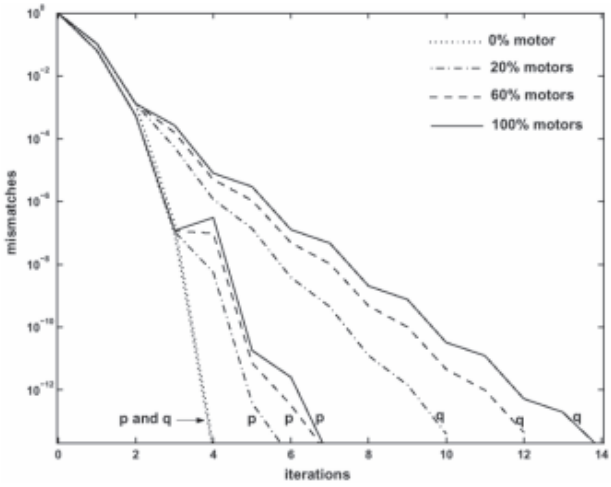

Figure 8. Active and reactive power mismatches of modified load flow with increased number of motors

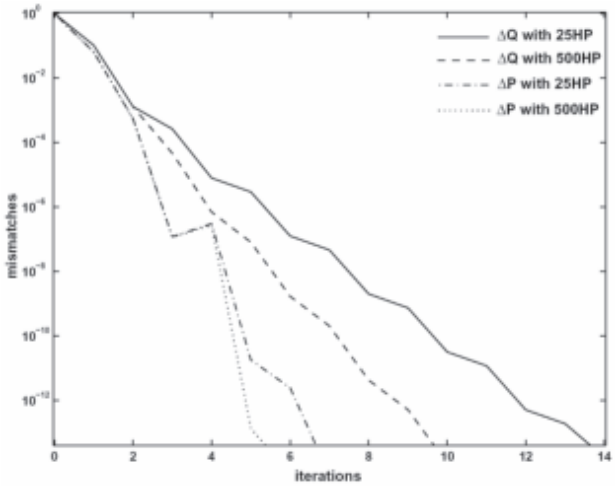

Figure 9. Active and reactive power mismatches of modified load flow with 25 and 500HP motors.

reactive power mismatch was more sensitive than that of the active power. The increase in the number of motors results in a slow convergence of reactive power mismatch due to the adjustments of the slip and scheduled reactive power. Hence more computational time of the modified load flow was required.

The convergence characteristics of the modified load flow were also tested with different ratings of motors, i.e., 25 and 500HP, which were either placed at bus 26. In the study, the total sum of the horsepower output of 25HP or 500HP motors was kept equally during the iteration process. The active and reactive power mismatches are displayed in Figure 9. The load flow solution with 500HP motors was converged faster than that of 25HP motors. Since 500HP motors operate at lower slip region, their reactive power consumptions are in fact lower than those of the 25HP motors at the same total HP output. Hence, less reactive power consumptions of the 500HP motor loads result in faster converged solution of load flow.

Conclusions

In this paper, the conventional load flow algorithm has been upgraded to incorporate the nonlinear model of induction motor load. The algorithm efficiency has been illustrated through the numerical example using the IEEE-30bus standard system. The upgraded algorithm is more advanced in providing a better way of initializing the induction motor because the exact amount of the motor reactive power consumption is obtained without any shunt compensation. However, incorporation of the motor nonlinear model into the load flow algorithm causes increases in the number of iterations since the reactive power mismatch slowly converges due to the slip and reactive power adjustments of motors during the iteration process. Moreover, increases in the number of motors and motor load buses result in an increased number of the iteration because of the motor nonlinear behavior.

Acknowledgement

The work described in this paper was sponsored by Thammasat University academic affairs, 2004.

References

IEEE Task Force. 1993. Load representation for dynamic performance analysis, IEEE Trans. Power Syst., 8: 472-482.

IEEE Task Force. 1995. Standard Load Model for Power Flow and Dynamic Performance Simulation, IEEE Trans. Power Syst., 10: 1302-1313.

Harley, R.G., Makram, E.B. and Duran, E.G. 1988. The effects of unbalanced networks and unbalanced faults on induction motor transient, IEEE Trans. Energy Conv., 2: 398-403.

Liu, Y., Lee, W. and Chen, M. 1997. Incorporating Induction Motor Model in a Load Flow Program for Power System Voltage Study, Electric Machines and Drives Conference Record, IEEE International Conference, TC3: 7.1-7.3.

Kundur, P. 1993. Power System Stability and Control, McGraw-Hill, New York.

Machowski, J., Bialek, J. and Bumby, J.R. 1997. Power System Dynamics and Stability, John Wiley & Sons, England.

Pereira, L., Kosterev, D., Mackin, P., Davies, D. and Undrill, J. 2002. An Interim Dynamic Induction Motor Model for Stability Studies in the WSCC, IEEE Trans. Power Syst., 17: 1108-1115.

Prasad, G. D. and Al-Mulhim, M. A. 1997. Performance Evaluation of Dynamic Load Models for Voltage Stability Analysis. Int. J. of Electr. Power Energy Syst., 19: 533-540.

Wallach, Y. 1986. Calculation and Programs for Power System Networks, Prentice-Hall, New York.

Appendix A: Load flow data (100MVA base)

Table A1. Line impedance and charging.

Between buses	Line parameters (pu)		
	R	X	B_c(total)
1-2	0.0192	0.0575	0.0528
1-3	0.0452	0.1852	0.0408
2-4	0.0570	0.1737	0.0368
3-4	0.0132	0.0379	0.0084
2-5	0.0472	0.1983	0.0418
2-6	0.0581	0.1763	0.0374
4-6	0.0119	0.0414	0.0090
5-7	0.0460	0.1160	0.0204
6-7	0.0267	0.0820	0.0170
6-8	0.0120	0.0420	0.0090
12-14	0.1231	0.2559	0
12-15	0.0662	0.1304	0
12-16	0.0945	0.1987	0
14-15	0.2210	0.1997	0
16-17	0.0824	0.1923	0
15-18	0.1073	0.2185	0
18-19	0.0639	0.1292	0
19-20	0.0340	0.0680	0
10-20	0.0936	0.2090	0
10-17	0.0324	0.0845	0
10-21	0.0348	0.0749	0
10-22	0.0727	0.1499	0
21-22	0.0116	0.0236	0
15-23	0.1000	0.2020	0
22-24	0.1150	0.1790	0
23-24	0.1320	0.2700	0
24-25	0.1885	0.3292	0
25-26	0.2544	0.3800	0
25-27	0.1093	0.2087	0
27-29	0.2198	0.4153	0
27-30	0.3202	0.6027	0
29-30	0.2399	0.4533	0
8-28	0.0636	0.2000	0.0428
6-28	0.0169	0.0599	0.0130

Table A2. Generators.

Bus no.	Voltage (pu)	Generation (MW)	Min. MVAR	Max. MVAR
1 (slack)	1.060	0		
2	1.043	40	-40	50
5	1.010	0	-40	40
8	1.010	0	-10	40
11	1.082	0	-6	24
13	1.071	0	-6	24

Table A3. Transformers.

Between buses	X (pu)	Tap
6-9	0.2080	0.978
6-10	0.5560	0.969
9-11	0.2080	1
9-10	0.1100	1
4-12	0.2560	0.932
12-13	0.1400	1
28-27	0.3960	0.968

Table A4. Shunt compensator.

Bus no.	G (pu)	B (pu)
10	0	0.19
24	0	0.043

Table A5. Loads.

Bus no.	MW	MVAR	Bus no.	MW	MVAR
1	0.000	0.000	16	3.500	1.800
2	21.70	12.70	17	9.000	5.800
3	2.400	1.200	18	3.200	0.900
4	7.600	1.600	19	9.500	3.400
5	94.20	19.00	20	2.200	0.700
6	0.000	0.000	21	17.50	11.20
7	22.80	10.90	22	0.000	0.000
8	30.00	30.00	23	3.200	1.600
9	0.000	0.000	24	8.700	6.700
10	5.800	2.000	25	0.000	0.000
11	0.000	0.000	**26**	P_m	Q_m
12	11.20	7.500	27	0.000	0.000
13	0.000	0.000	28	0.000	0.000
14	6.200	1.600	29	2.400	0.900
15	8.200	2.500	30	10.60	1.900

Appendix B: Induction machine parameters (based on own horsepower output)

HP	R_s	R_r	X_{ls}	X_{lr}	X_m	N_r	Pole	f (Hz)	Volt
25	0.0219	0.0472	0.0498	0.0498	1.9504	1695	4	60	460
500	0.0185	0.0132	0.0851	0.0851	3.8092	1773	4	60	2300